Optica Applicata, Vol. XII, No 3-4, 1982

Size-sensitive filters

D. EBERLEIN, A. SCHWERDTNER

Ingenieurhochschule Dresden, 8019 Dresden, Hans-Grundig-Str. 25, DDR.

An approach is investigated for obtaining spatial frequency filters which are highly sensitive to variations in size, shape, and orientation of objects. The filter effects a phase change of the incident object wave and is strongly dependent on the object expected in the input plane. For real symmetric objects the filters become simple phase masks.

1. Introduction

A lot of filters, employed in recognition procedures using coherent light, have come to be known from the literature [1-3]. The locations of the objects are then indicated by light intensity peaks in the output plane. Figure 1 depicts a scheme of a potential filtering setup.

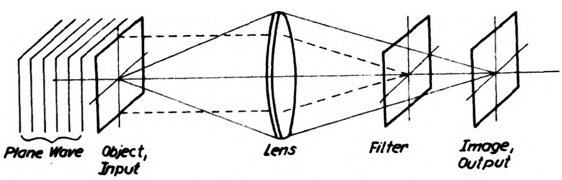

Fig. 1. Fourier transform filtering setup

In many cases a matched filter [4-6] would be the most suitable. These filters are, however, insensitive with respect to the size of object, while this property is often of interest, for instance, in character recognition. If to the given object another part is added which does not overlap the object, the peak does not change at all, provided the same filter is used. On the other hand, the inverse filter [7] would be best fitted to the problem of sizing the objects. The filtered object would then appear in the image plane as a very narrow peak, like a Dirac δ-function, spread somewhat due to the finite size of the Fourier transform. Small changes in the size or shape of the object result then in a rapid decrease of the peak. Unfortunately, such a filter function is hard to realize due to the poles of the function. This means that the filter contains only the values corresponding to the zero-crossing points of the Fourier transform of the object.

Spatial frequency filters for sizing circular objects performing simple phase changes 0 and π [8] were suggested several years ago. Similarly to inverse filters, such filters proved to be very sensitive to size variations, as was shown by experimental investigations. The filter reverses the sign of the bipolar spectrum in such a way that the amplitude leaving the filter takes on only nonnegative values. The filter material used was the so-called Veotograph film.

We found this approach of making filters useful for detecting small object variations in general, i.e., changes in size, shape, and orientation. For this reason we studied this method by computational and experimental investigations and compared the results with those obtained when matched filters were used. As objects we used circles the diameters of which were varied. In this way the efficiency of the filters in sizing objects could be shown. As filter material we used photo resist.

Further we suggest to extend this approach to arbitrary complex-valued Fourier transforms of objects by the use of synthetic holograms as phase compensating filters.

In Section 2 the approach of size-sensitive filters is presented in a more general manner. Section 3 covers computational considerations as well as experimental results.

2. Size-sensitive filter (SSF)

The approach of SSF may be best presented by using a simple example [8, 9]. Let the object be a circular aperture in the front focal plane of a lens

$$O(r) = \mathrm{circ}(r/a) = \begin{cases} 1, & r \leqslant a, \\ 0, & \text{else.} \end{cases} \tag{1}$$

The amplitude distribution in the back focal plane of the lens may then be described as a Fourier transform (FT)

$$\tilde{O}(\rho) = \pi a^2 \frac{2J_1(2\pi\rho a)}{2\pi a\rho}, \tag{2}$$

where ρ denotes the spatial frequency in the radial direction and J_1 is the Bessel function of the first order.

Figure 2a shows the map of $\tilde{O}(\rho)$ continued symmetrically. The function $\tilde{O}$ suffers a phase change π at the zeros of the J_1-function. The filter function (Fig. 2b) has phase reversals at the same locations. After passing the filter the amplitude distribution may be described by its modulus $|\tilde{O}|$ (Fig. 2c).

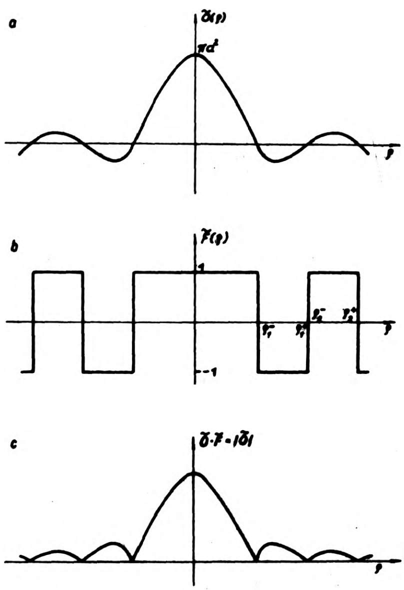

Fig. 2.a. FT of a circ-function.
b. Filter function,
c. Amplitude leaving the filter

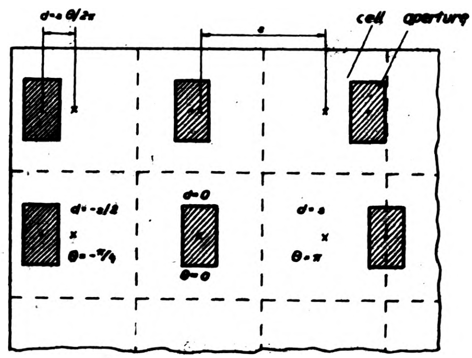

Fig. 3. Synthetic hologram for making SSF

This function is then Fourier-transformed in the image plane (Fig. 1). For a central object the peak appears on the optic axis of the image plane, i.e., $r = 0$. We, therefore, obtain as peak amplitude in the image plane the Fourier transform $|\tilde{O}|$ at $r = 0$, which in polar coordinates takes simply the form

$$B(0) = 2\pi \int_0^{\rho_N} |\tilde{O}(\rho)|\rho d\rho. \tag{3}$$

This means the sum of all contributions of the annular regions defined by the zeros of $\tilde{O}$, from this it easily follows that such a filter gives the highest possible amplitude as well as the intensity in the peak.

If the object is varied slightly in size or shape Eq. (3) does not hold any longer. The peak amplitude decreases. Due to the invariance of spatial frequency filters with respect to shifting objects, off-axis locations of objects result in off-axis locations of the peak.

The intensity represents a very important quantity in the filtering process for at least two reasons, The first one has just been discussed with respect to the sensitivity to size variation. But no less important is the quality of a filter with respect to the diffraction efficiency. By diffraction efficiency we mean the light energy related to the energy incident on the object. This filter is readily seen to have the largest possible diffraction efficiency with the energy concentrated in the peak. Its amount depends on the extension ρ_N of the filter. This is shown more extensively in the next Section.

The generalization of SSF applied to complex-valued Fourier transforms is straight forward. The modulus of the filter function must be constant and should be chosen as large as possible so as to obtain the maximum diffraction efficiency. The phase distribution of the filter has to be fitted in such a way that it compensates the phase distribution of the FT O of the object. Filters of this type may be made by means of synthetic holography.

Using, for instance, Lohmann's concept [7] one has to divide a non-transparent mask into equally spaced cells (Fig. 3). The spacing S cannot be chosen too large in order to avoid the overlapping of adjacent diffraction orders which will occur when synthetic hologram is used. Given the distance D between two diffraction orders in the image plane, the spacing S of the hologram cells has to be at least $\lambda F/D$, where λ is the wave length, and F – the focal length of the lens used. Each cell contains an aperture of uniform size and shape, for instance, rectangular. The dislocation d of the aperture in a cell corresponds to the phase θ that compensates for the phase φ of the Fourier transform $\tilde{O} = |\tilde{O}| \exp_{(j\varphi)}$ at this point, that is $\varphi = -\theta$. In each cell the phase is proportional to the shift of the aperture from the centre of the cell. The phases π and $-\pi$ are obtained for apertures located at the edges of the cells.

There are a lot of other types of synthetic hologram [10, 11]. The so-called kinoforms are especially suited owing to their high diffraction efficiency using the zeroth diffraction order [12].

3. Computational and experimental results

In order to get a better insight into the approach of SSF we have performed several computations and obtained numerical results. We started with determining spatial frequencies $\rho_n^{\pm}$ of the annular zones of a given SSF, that is, we calculated the zeros of Eq. (2). The transmittance of the zones n may be described by $(-1)^n$, see Fig. 2b. Then, using the relation

$$B(r) = 2\pi \sum_{n=0}^{\infty} (-1)^n \int_{\rho_n^-}^{\rho_n^+} \left(b^2 \pi \frac{2J_1(2\pi\rho b)}{2\pi\rho^{h}} \right) J_0(2\pi\rho r)\rho d\rho \qquad (4)$$

we computed the output by means of Simpson's formula. The effect of the given SSF is represented by the factor $(-1)^n$ and the zone borders $\rho_n^{\pm}$. The first term in the integral describes the Fourier transform of the object with the radius b (instead of a) chosen for constructing the SSF.

Putting $b = a$ in the above equation we got the peak shape for the fitted SSF (Fig. 4). In similar way we computed the output using matched filter (MF). The output of an object filtered with a fitted SSF shows a very narrow and very high peak. The same is true for the intensities, but then the peak of Fig. 4 cannot be mapped.

As may be seen from Fig. 2 the amplitude as well the intensity in the peak increase with the extension of SSF. This is due to the fact that the area of the zones increases though the modulus $|\tilde{O}|$ of the impinging object wave decreases. For the object discussed the increase of the peak intensity is shown to be linear with respect to the SSF extent (Fig. 5).

The strong dependence of both the peak width and the peak height on the radius b may be understood also from a convolution point of view. In the image plane there occurs an amplitude distribution which is a convolution

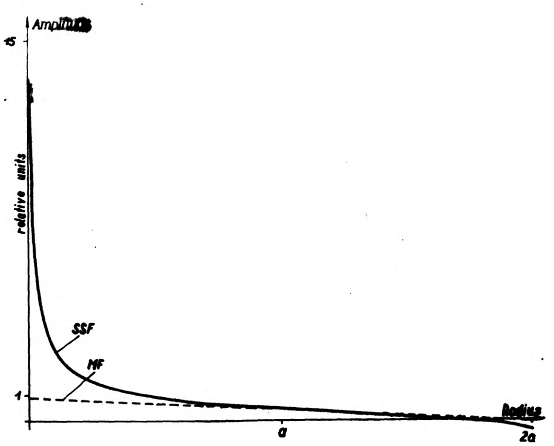

Fig. 4. Peak shape

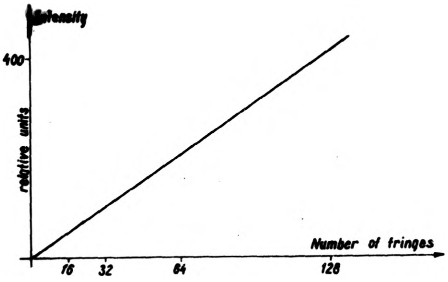

Fig. 5. Increase of peak intensity vs. the number of fringes

of the object with the filter response (Fig. 6). By filter response we mean the Fourier transform of the filter. In the case when the object is centred exactly within the filter response, large positive values contribute to the peak. The situation changes drastically if the object is shifted slightly across the filter response in the con-

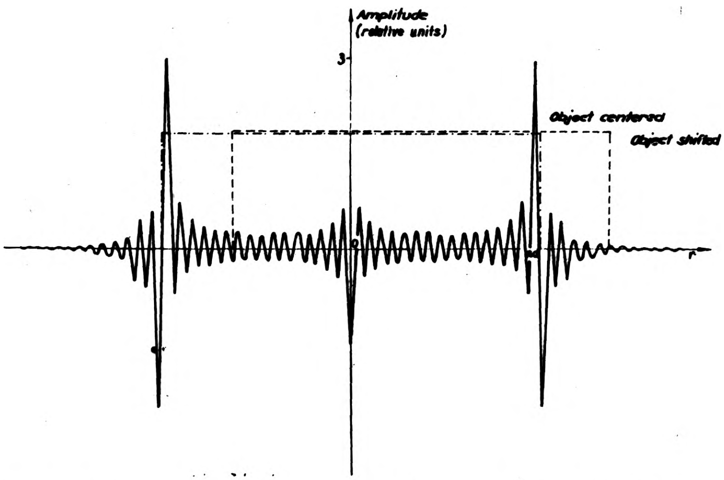

Fig. 6. Illustration to convolution (continued symmetrically)

volution process. Contributions of very large negative values as well as the loss of large positive values result in a sharp decrease of the peak. Figure 7 displays a photograph of the filter response. One of the most important questions arising is due to the sensitivity of the filter to size variations.

Figure 8 shows the dependence of matched filter (MF) and SSF on variations of the radius b of the circular object. The theoretical SSF curve was computed using Eq. (4), with $r = 0$. Notice that SSF are

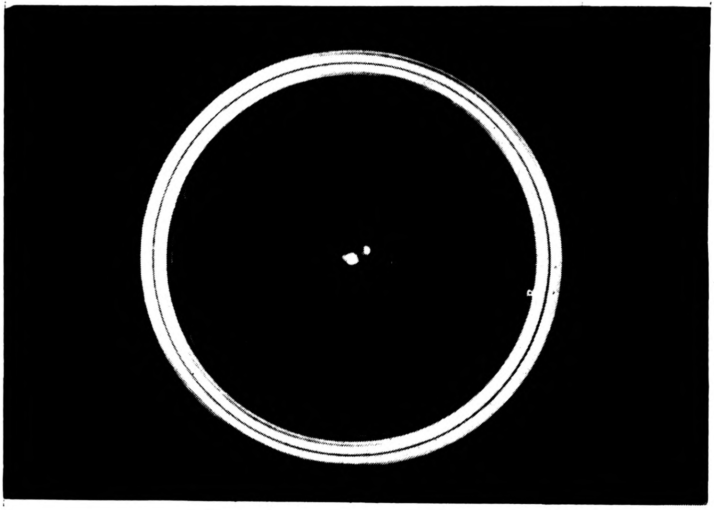

Fig. 7. Filter response of SSF

able to distinguish objects of sizes smaller and larger than the proper ones. Matched filters are only sensitive to smaller circular objects. The strong dependence of SSF on size variations compared to MF is also remarkable. The difference between theoretically predicted and experimentally obtained values is also due to this feature. Nevertheless, the measured SSF values lie clearly below the theoretical MF curve.

In concluding this Section we show the dependence of the shape of peak on the variations of the object size. Figure 9 shows a photograph of the peak corresponding to the SSF curve in Fig. 4.

Figures 10a and 11a show the peak shape using objects with radius $b = a + \Delta a$, computed with the help of Eq. (4). Figures 10b and 11b show photographs of the registered intensities. The obscuration in the centre of the peak is clearly seen.

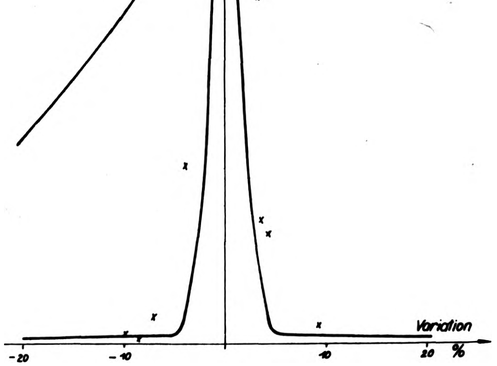

Fig. 8. Dependence of peak intensities on size variations

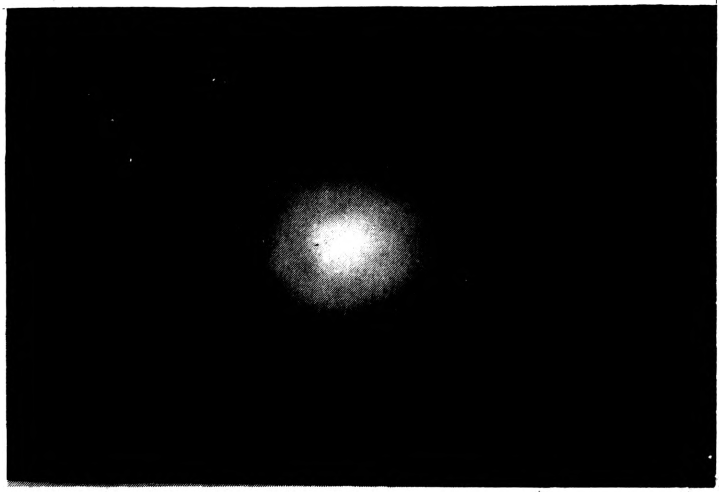

Fig. 9. Photograph of a peak for a SSF fitted to the object

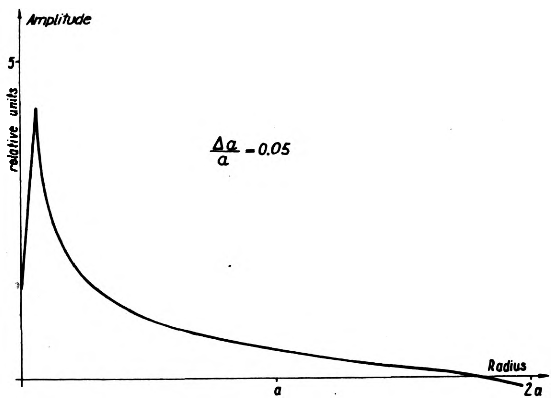

Fig. 10a.

4. Conclusion

The concept of size sensitive filters was shown to be very sensitive in sizing objects. The same sensitivity of size sensitive filters applies also to variations in shape or orientation. Beside the strong dependence on object variations, size sensitive filters are able to

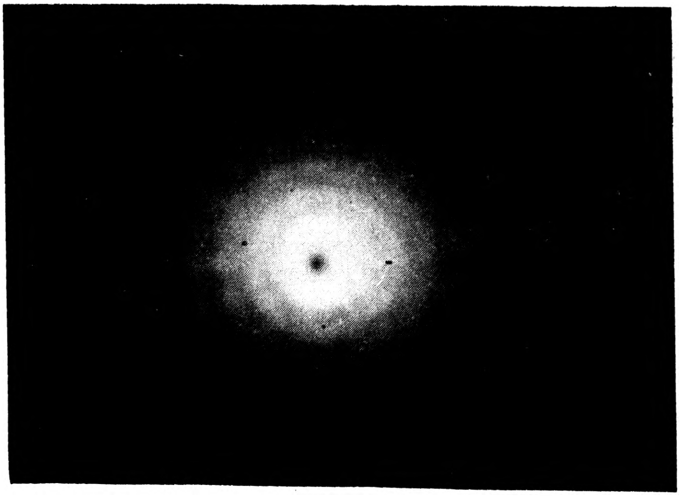

◀ Fig. 10b

Fig. 10. Peak shape for increased object (Fig. 10a) and photograph (Fig. 10b)

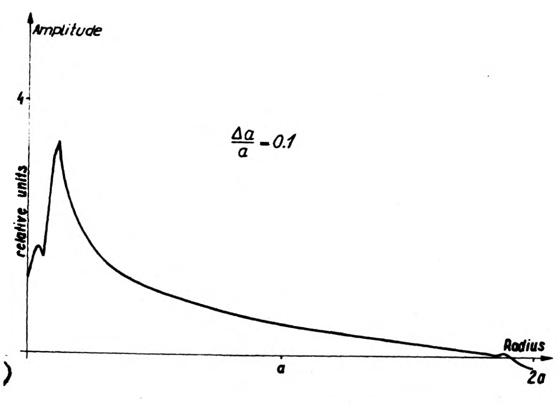

Fig. 11a

◀ Fig. 11b

Fig. 11. Similar to Fig. 9, but the size of object is further increased

discriminate between objects which cannot be distinguished by matched filters at all.

For arbitrary objects size sensitive filters may be made using synthetic holograms. In the case of real symmetric objects the filter simply becomes a bipolar phase mask.

References

[1] LEE W.H., Appl. Opt. 13(1974), 1677.
[2] SIROHI R.S., RAM MOHAN V., Optica Acta 24 (1977), 1105.
[3] CAULFIELD H.J., Appl. Opt. 19 (1980), 181.
[4] VANDER LUGT, Optica Acta 15 (1968), 1.
[5] GOODMAN J., Introduction to Fourier Optics, McGraw-Hill Book Co., San Francisco 1968.
[6] TURIN G.T., An Introduction to Matched Filters, IRE Trans. on Inf. Theory, 1960, 11.
[7] LOHMANN A.W., PARIS D.P., Appl. Opt. 7 (1968), 651.
[8] HOLLADAY T.M., GALLATIN J.D., J. Opt. Soc. Am. 56 (1966), 869.
[9] PARRENT G.B., WARD J.H., Optical Detection of Geometric Configuration. US Patent No. 411 8107, IC G 02 B 5181.
[10] LEE W.H., Progr. Opt. 16 (1978), 121.

[11] SCHWERDTNER A., Binäres Phasenhologramm mit beliebiger Übertragungsfunktion. GDR Patent No. 205738, IC G 03 H.

[12] LESEM L.B., HIRSCH P., JORDAN J.A., IBM J. Res. Develop. 13 (1969), 150.

Received June 22, 1981
in revised form December 22, 1981

ФИЛЬТРЫ, ЧУВСТВИТЕЛЬНЫЕ К РАЗМЕРАМ

Были исследованы возможности получения фильтров пространственных частот, чувствительных к изменениям размеров, формы, а также ориентации предметов. Эти фильтры вызывают изменение фазы падающей предметной волны и сильно зависят от предмета, ожидаемого во входной плоскости. Для реальных асимметрических предметов фильтр становится просто биполярной фазовой маской.